



The Society for engineering  
in agricultural, food, and  
biological systems

This is not a peer-reviewed article.

Paper Number: 033138

An ASAE Meeting Presentation

## Determination of durum wheat vitreousness using transmissive and reflective images

Ning Wang, Assistant Professor, Department of Bioresource Engineering, McGill University,  
Quebec, Canada

Naiqian Zhang, Professor, Department of Biological and Agricultural Engineering, Kansas  
State University, Manhattan, Kansas, USA

Floyd Dowell, Research Leader, Grain Marketing and Production Research Center, ARS,  
USDA, Manhattan, Kansas, USA

Tom Pearson, Research Scientist, Grain Marketing and Production Research Center, ARS,  
USDA, Manhattan, Kansas, USA

Written for presentation at the  
2003 ASAE Annual International Meeting  
Riviera Hotel and Convention Center  
Las Vegas, Nevada, USA  
July 27- July 30, 2003

**Abstract.** *Digital imaging technology has found many applications in grain industry. In this study, images of durum wheat kernels acquired under three illumination conditions - reflective, side-transmissive, and transmissive - were used to develop artificial neural network (ANN) models to classify durum wheat kernels by their vitreousness. The results showed that the models trained using transmissive images provided the best classification for the nonvitreousness class - 100% for non-vitreous kernels and 92.6% for mottled kernels. Results of the study also indicated that, using transmissive illumination may greatly reduce the hardware and software requirements for the inspection system, while providing faster and more accurate results, for inspection of vitreousness of durum wheat.*

**Keywords.** Grading, Inspection, Automation, Machine Vision, Color

---

The authors are solely responsible for the content of this technical presentation. The technical presentation does not necessarily reflect the official position of the American Society of Agricultural Engineers (ASAE), and its printing and distribution does not constitute an endorsement of views which may be expressed. Technical presentations are not subject to the formal peer review process by ASAE editorial committees; therefore, they are not to be presented as refereed publications. Citation of this work should state that it is from an ASAE meeting paper. Ning Wang, 2003. Determination of durum wheat vitreousness using transmissive and reflective images. ASAE Meeting Paper No. 033138. St. Joseph, Mich.: ASAE. For information about securing permission to reprint or reproduce a technical presentation, please contact ASAE at [hq@asae.org](mailto:hq@asae.org) or 616-429-0300 (2950 Niles Road, St. Joseph, MI 49085-9659 USA).

---

## Determining durum wheat vitreousness using transmissive and reflective images

Ning Wang  
Member

Naiqian Zhang  
Member

Floyd Dowell  
Member

Tom Pearson  
Member

### Introduction

As a major class of wheat, durum (*Triticum turgidum* L. Var durum) production accounts for approximately 8% of the wheat production worldwide (Abaye *et al*, 1997). Durum wheat is mainly used to make semolina for macaroni, spaghetti, and other pasta products. The best durum wheat for pasta products should appear hard, glassy and translucent, and have excellent amber color, good cooking quality, and high protein content. Nonvitreous (starchy) kernels are opaque and softer, and result in decreased yield of coarse semolina. Thus, vitreousness of durum wheat has been used as one of the major quality attributes in grading.

Traditionally, grain grading has been primarily done by visual inspection of trained personnel. This method is subjective and tedious. It also produces great variations in inspection results between inspectors. Targeting on the disadvantages of human inspection, many researches have been conducted to develop objective, rapid, and automated grain-grading systems.

Various methods to detect vitreousness of durum wheat kernels were investigated. Dowell (2000) reported perfectly matched classification results between a single-kernel NIR spectroscopy method and human inspectors on obviously vitreous and nonvitreous durum wheat kernels. Sissons *et al.* (2000) used a commercial single-kernel characterization system (SKCS 4100, Perten Instruments, Springfield, IL) to predict semolina mill yield of durum wheat kernels based on vitreousness. As a fast developing technology, machine-vision-based systems have shown great potential on accessing grain physical conditions. Many researchers combined image acquisition, processing, and analysis techniques with advanced classification algorithms, including statistical analysis and artificial neural network (ANN), to detect grain kernel features, such as color, texture, and various types of damages (Zayas *et al*, 1994; Luo *et al*, 1999; Ruan *et al*, 2001; Bacci *et al*, 2002). Symons *et al* (2001) developed a machine-vision based system to classify durum wheat kernels according to the degree of vitreousness. Their results were highly consistent with those from human inspection. In a previous study, we developed neural-network models based on *reflective* kernel images to determine the vitreousness of durum wheat using a real-time, image-based wheat quality inspection machine, the GrainCheck 310 (FOSS Tecator, Höganäs, Sweden). The correct classification for vitreousness kernels reached 85-90% (Wang *et al.*, 2003).

Vitreousness is the nature of an object that resembles glass in transparency, brittleness, hardness, and glossiness (The American Heritage® Dictionary, 2000). A glass differs from an opaque object not only in its ability to reflect light, it also differ in its ability to transmit light. A common-sense perception of vitreous kernels is that they would allow much more light to

transmit than would non-vitreous kernels. Thus, images of kernels taken with *transmissive* light may carry more information on kernel vitreousness. This study was based on this common-sense perception. The objective of this study was to compare the effectiveness of determining the vitreousness of durum wheat using transmissive and reflective kernel images.

## **Materials and procedures**

### Sample preparation

The Grain Inspection, Packers, and Stockyards Administration (GIPSA) of USDA provided test samples for this study. The samples were classified as “hard vitreous and of amber color” (HVAC) or “not hard vitreous and of amber color” (NHVAC) by visual inspection of the Board of Appeals and Review (BAR). A sub-class of NHVAC, “mottled/chalky durum kernels inspected as NHVAC” (mottled), was also used. Sample of each class weighed 100g. Before the experiment, 500 kernels were randomly selected from each class to be used as the calibration sample set. 500 kernels also were randomly selected from each class to form a validation sample set. The calibration set was used to train ANN models, whereas the validation set was used to test the model performance.

### Image acquisition

Three images were taken for each kernel: reflective image, side-transmissive image, and transmissive image. The reflective and side-transmissive images were taken using a commercial, image-based grain-inspection system. The system uses a CMOS camera with a resolution of 640×480 pixels/image and 24 bits color. The distance between the camera and the kernel was 10cm. For the reflective images, two 24-LED panels were used to provide white light illumination (Figure 1(a)). The side-transmissive images used two LEDs positioned at two ends of a cavity, in which the kernel was placed. The LED is red in color with a peak wavelength at 660nm and a view angle of 100 degree. The camera used for the side-transmissive images was the same as the one used for the reflective images. The distance between the camera and the kernel was also 10cm (Figure 1(b)).

The transmissive images were taken using a back-light image acquisition system. The kernel was placed on a glass surface. Incandescent light was placed underneath the glass and was directed upwards. The camera used was a simple, board-level CCD camera with a spatial resolution of 640×480 pixels. The distance between the camera and the kernel was 12.5cm. A schematic drawing of the image acquisition system is shown in Figure 1(c). Examples of reflective, side-transmissive, and transmissive images for HVAC, NHVAC, and mottled kernels are shown in Figure 2.

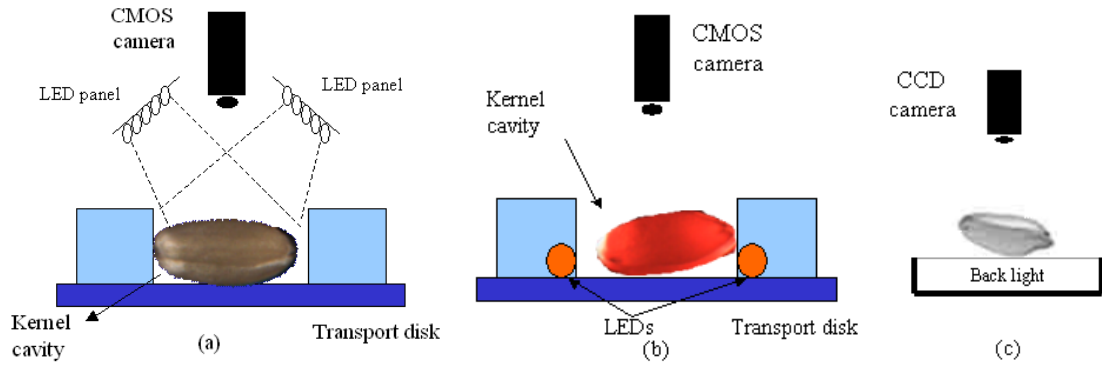


**Figure 1. Image acquisition systems for: (a) reflective images, (b) Side-transmissive images, and (c) transmissive images**

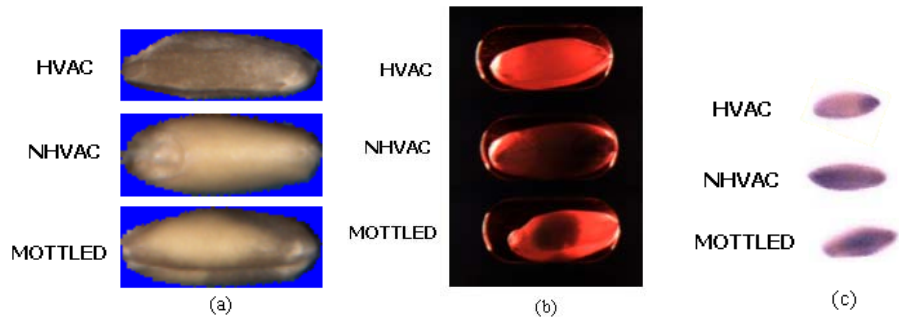


**Figure 2. Images of HVAC, NHVAC, and Mottled kernels: (a) reflective, (b) side-transmissive, and (c) transmissive**

Feature extraction

Four global features and two types of distribution features, each containing 50 elements, were extracted from each kernel image. Thus, the total number of features used as the inputs to an ANN classification model was 104. The four global features are: 1) Sum of the number of rows and the number of columns of the image containing the kernel, 2) Sum of sin(hue) of all pixels in the image, 3) Sum of cos(hue) of all pixels in the image, and 4) Average intensity of the image.

The 100 distribution features came from two histograms for each image. The first is the histogram for intensity. The intensity range between 50 and 255 was evenly divided to 50 intervals. The numbers of pixels with intensity values falling into each interval were used as the distribution features. Similarly, the histogram for hue of the same image was used to produce the other 50 features. The 50 equal intervals were derived from the entire range of hue - from 0 to  $2\pi$ .

## Artificial Neural Network (ANN)

A back-propagation network architecture with one hidden layer was used in this study (Figure 3). The 104 features extracted from each image were the inputs of the ANN, whereas the number of outputs was equal to the number of classes to be classified. In the network, nodes on adjacent layers are fully connected with weights. These weights were adapted through calibration of the training data in a step-wise manner by repeatedly presenting the data to the ANN for a number of epochs so as to minimize the classification errors. Once the weights were determined, the ANN could be used to categorize samples that were not included in the calibration process.

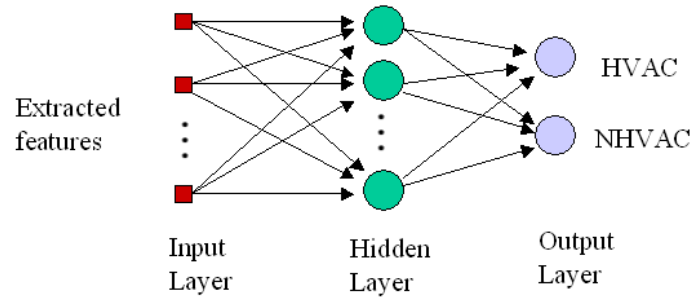


**Figure 3. Structure of the ANN**

ANN calibration models with 20 hidden layer nodes were developed for the three types of kernel images. The classification rates for each type of kernels as defined in Equation (1) were evaluated and compared:

$$\text{Classification rate for class } A = \frac{\text{Number of kernels classified to class } A \text{ by an ANN classifier}}{\text{Total number of kernels in a sample labeled class } A \text{ by BAR}} \quad (1)$$

## Experiment Design

Two sets of experiments were conducted. Both experiments were intended to compare the effectiveness of three calibration models developed using images acquired under different illumination conditions – reflective, side-transmissive, and transmissive - in classifying vitreous from non-vitreous kernels. The only difference between the two experiments was that, for Experiment 1, samples of only two classes - HVAC and NHVAC – were used, whereas for Experiment 2, mottled kernels were used as a part of non-vitreous kernels (NHVAC class) in both calibration and validation.

### Experiment 1

500 images taken from each of the HVAC and NHVAC samples were used to establish ANN calibration models. As mentioned earlier, 104 features were used as inputs of the ANN. Two

classes, HVAC and NHVAC, were the output of the ANN. The classification results were compared among the models established using three types of images, reflective, side-transmissive, and transmissive. The numbers of kernel images used for validation were the same.

### Experiment 2

Mottling is a small, non-vitreous area within a kernel. Thus, mottled kernels are considered non-vitreous. For most mottled kernels, however, mottling occurs only on a portion of the kernel, and other areas on the same kernel may appear vitreous. Due to the randomness in orientation when kernels are placed in front of the camera, mottled areas may not always be exposed to the camera's field of view. When images taken were of the reflective type, a considerable amount of mottled kernels can be viewed by the camera as vitreous kernels. Transmissive illumination, on the other hand, reflects the amount of light passing through the kernel. Thus, the effect of kernel orientation may impose a lesser problem for identification of mottled kernels using transmissive images.

Experiment 2 used the same 500 images of HVAC kernels for calibration. For the NHVAC class, only 250 samples were randomly selected from the 500 kernels used in Experiment 1. Added to the NHVAC sample were 250 images of randomly selected mottled kernels. Identical numbers of kernels were used in validation. The 104 features were again used as the inputs to the ANN. Two classes, HVAC and NHVAC, were defined as the outputs of the ANN. The classification rate for the mottled class was defined as the number of mottled kernels classified into the NHVAC class divided by the total number of mottled kernels. The classification results were again compared among the models established using three types of images: reflective, side-transmissive, and transmissive.

## **Results and Discussion**

### Experiment 1

Calibration results of the prediction models with 20 hidden layer nodes using reflective image, side-transmissive image, and transmissive image, showed quite similar classification rates (Table 2). Table 3 shows the validation results using the validation data set. The model based on transmissive images provided perfect classifications for both HVAC and NHVAC classes. The model using side-transmissive images had higher classification rates of 97.3% and 85.1% for HVAC and NHVAC, respectively, compared with those from the model using reflective images.

**Table 2. Calibration results**

	Classification rate (%)	
	HVAC	NHVAC
Prediction Model using reflective image	100	100
Prediction Model using side-transmissive image	100	98.5
Prediction Model using transmissive image	100	100

**Table 3. Validation results**

	Classification rate (%)	
	HVAC	NHVAC
Prediction Model using reflective images	93.8	80.3
Prediction Model using side-transmissive images	97.3	85.1
Prediction Model using transmissive images	100	100

Experiment 2

For the calibration data set, the models established using the reflective and side-transmissive images had similar performance. The model using the transmissive images, on the other hand, had perfect classifications for both classes (Table 4). The ANN model was validated using the validation set with HVAC, NHVAC, and Mottled classes. Table 5 shows the validation results. The models based on transmissive images showed an apparent improvement on the classification of mottled and NHVAC classes. When reflective images were used, only 63% of the mottled kernels were classified as NHVAC. When side-transmissive images were used, the classification rate improved to 83.3%. It was further improved to 92.9% when the transmissive images were used. Meanwhile, the classification rate for the NHVAC class was also improved from 82% to 94.3% for the side-transmissive images and to 100% for the transmissive images. Apparently, the effect of kernel orientation on classification for mottled kernels was largely eliminated with the transmissive setup of the illumination.

**Table 4. Calibration results**

	Classification rate (%)	
	HVAC	NHVAC+Mottled
Prediction Model using reflective	94.7	89.5
Prediction Model using side-transmissive	94.7	92.2
Prediction Model using transmissive	100	100

**Table 5. Validation results**

	Classification rate (%)		
	HVAC	NHVAC	Mottled
Prediction Model using reflective images	88.0	82.0	63.3
Prediction Model using side-transmissive	87.4	94.3	83.3
Prediction Model using transmissive	91.6	100	92.9

Results from the two experiments also showed that the types of images used to train ANN models did not have significant effect on the classification rate for the HVAC class. The use of transmissive illumination mainly improved classification of the NHVAC class, including the mottled class. With the advantages of transmissive images, further study can be conducted to

reduce the image features used (probably complete remove the spatial features) and to simplify the algorithm in the classification models. A simpler statistical analysis algorithm, such as discriminant analysis, may be used for faster classification. Furthermore, the use of transmissive images may also allow the reduction of hardware requirements for the system. The camera used for collecting transmissive images in this study was a low-cost camera with low spatial and color resolutions. This would greatly reduce the cost of the inspection system.

## **Summary**

Three types of kernel images - reflective, side-transmissive, and transmissive - were collected using two image acquisition systems. 104 features were extracted from the images. The features were used as the inputs for an artificial neural network, which classified the kernels into two classes: HVAC and NHVAC.

Two experiments were conducted to compare the effectiveness of the ANN models established using three types of images – reflective, side-transmissive, and transmissive. In the first experiment, only HVAC and NHVAC samples were used. The validation results showed that the model based on transmissive images provided perfect classifications for both the HVAC and NHVAC classes. The model using side-transmissive images provided a better classification rates than the model using reflective images.

In the second experiment, mottled samples were added to the NHVAC class to train the ANN models. The output classes of the ANN were still HVAC and NHVAC. The validation results indicated a great improvement in classifying the molted kernels using transmissive illumination. The classification rates for mottled kernels using transmissive images reached 92.9%, compared to 83.3% using side-transmissive images and 63.3% using reflective images. On the other hand, use of transmissive illumination did not show significant impact on classification of the HVAC kernels.

Results of the study also indicated that, using transmissive illumination may greatly reduce the hardware and software requirements for the inspection system, while providing faster and more accurate results, for inspection of vitreousness of durum wheat.

## References

Abaye, A.O., D.E. Brann, M.M. Alley, C.A. Griffey, 1997. Winter Durum Wheat: Do We Have All the Answers? *Virginia Tech Publication*, page: 424-802.

Bacci, L., B. Rapi, F. Colucci, and P. Novaro, 2002. Durum Wheat Quality Evaluation Software. *Proceedings of the World Congress of Computers in Agriculture and Natural Resources*, 13-15, March 2002, Iguacu Falls, Brazil, pp. 49-55.

Dowell, F.E. 2000. Differentiating vitreous and nonvitreous durum wheat kernels by using near-infrared spectroscopy. *Cereal Chemistry*. 77(2): 155-158.

Luo, X., D.S. Jayas, and S. J. Symons, 1999. Identification of Damaged kernels in wheat using a color machine vision system. *J. Cereal Science*. 30(1999): 49-59.

Ruan, R., S. Ning, L. Luo, P. Chen, R. Jones, W. Wilcke, and V. Morey, 2001. Estimation of Weight percentage of scabby wheat kernels using an automatic machine vision and neural network based system. *ASAE Transactions*. 44(4): 983-988.

Sissons, M.J., B.G. Osborne, R.A. Hare, S.A. Sissons, and R. Jackson. 2000. Application of the single-kernel characterization system to durum wheat testing and quality prediction. *Cereal Chemistry*. 77(2): 4-10.

Symons, S.J., L. Van Schepdael, and J.E. Dexter, 2001. Measurement of hard vitreous kernels in durum wheat by machine vision. *J. Cereal Science*. In press.

The American Heritage® Dictionary of the English Language, Fourth Edition. 2000 by Houghton Mifflin Company. Published by Houghton Mifflin Company.

Wang, N., F.E. Dowell, and N. Zhang, 2003. Determining wheat vitreousness using image processing and a neural network. *Transactions of ASAE*. 46(4).

Zayas, I.Y, D. B. Bechtel, J.D. Wilson, and E. E. Dempster, 1994. Distinguishing selected hard and soft red winter wheats by image analysis of starch granules. *Cereal Chemistry*. 71(1): 82-86.